TITLE:

Effect of Graphite Orientation and Lithium Salt on Electronic Passivation of Highly Oriented Pyrolytic Graphite

AUTHOR(S):

Tang, Maureen; Miyazaki, Kohei; Abe, Takeshi; Newman, John

CITATION:

Tang, Maureen ...[et al]. Effect of Graphite Orientation and Lithium Salt on Electronic Passivation of Highly Oriented Pyrolytic Graphite. Journal of The Electrochemical Society 2012, 159(5): A634-A641

ISSUE DATE:

2012-03-05

URL:

http://hdl.handle.net/2433/193702

RIGHT:

© The Electrochemical Society, Inc. 2012. All rights reserved. Except as provided under U.S. copyright law, this work may not be reproduced, resold, distributed, or modified without the express permission of The Electrochemical Society (ECS).

京都大学学術情報リポジトリ
KURENAI
Kyoto University Research Information Repository

京都大学 KYOTO UNIVERSITY
A Self-archived copy in
Kyoto University Research Information Repository
https://repository.kulib.kyoto-u.ac.jp
京都大学学術情報リポジトリ KURENAI 紅 Kyoto University Research Information Repository

Journal of The Electrochemical Society, **159** (5) A634-A641 (2012)
0013-4651/2012/159(5)/A634/8/$28.00 © The Electrochemical Society

Effect of Graphite Orientation and Lithium Salt on Electronic Passivation of Highly Oriented Pyrolytic Graphite

Maureen Tang,[a,b,*,z] Kohei Miyazaki,[c,] Takeshi Abe,[c,**] and John Newman[a,b,***]**

[a]*Department of Chemical and Biomolecular Engineering, University of California, Berkeley, California 94720-1462, USA*
[b]*Environmental Energy Technologies Division, Lawrence Berkeley National Laboratory, Berkeley, California 94720, USA*
[c]*Graduate School of Engineering, Kyoto University, Kyoto 615-8510, Japan*

This work studies the effect of edge-to-basal plane ratio on the macroscopic formation kinetics and electrochemical properties of the solid-electrolyte-interphase (SEI). The relative fraction of edge and basal planes was calculated by measuring the double-layer capacitance of highly oriented pyrolytic graphite (HOPG) in 1.0 M KCl. The formation kinetics was studied using chronoamperometry (CA) and cyclic voltammetry (CV). The electrochemical properties of the SEI were studied by CV and electrochemical impedance spectroscopy (EIS) of ferrocene. Results show that, as expected, current due to both lithium intercalation and SEI formation increases with the fraction of edge planes. After SEI formation in $LiClO_4$-based electrolyte, the edge plane permits slightly more electron transfer to ferrocene. Attempts to form the SEI incompletely by running CV scans to progressively lower voltages show that oxygen contamination produces a more passivating SEI. Ferrocene CV shows that the SEI formation causes mass-transport limitations by either formation of a porous layer or blocking the active area of the electrode, but the kinetics of the ferrocene reaction remains fast even in the presence of the SEI. Comparison of formation CVs for $LiPF_6$- and $LiClO_4$-based electrolytes shows that HOPG passivates much more rapidly with $LiClO_4$.
© 2012 The Electrochemical Society. [DOI: 10.1149/2.073205jes] All rights reserved.

Manuscript submitted December 5, 2011; revised manuscript received February 6, 2012. Published March 5, 2012.

Growth of the solid electrolyte interphase, or SEI, is known to be a major cause of capacity fade in lithium-ion batteries. Because of the complexity of the chemistry involved in SEI formation reactions, the mechanism by which an SEI succeeds or fails to passivate the graphite electrode is still not understood. One difficulty in studying the SEI is a lack of in-situ characterization techniques. Measuring capacity fade by repeated cycling or prolonged storage is very slow, and the irreversiblity of formation reactions makes analysis of transport and kinetics difficult. Adding the ferrocene redox couple to electrolyte and measuring through-film kinetics provides an alternative method of studying the SEI. This method is advantageous because the fast kinetics in the absence of any surface films provide a clear comparison for behavior on a passivated electrode. Furthermore, the high oxidation potential ($E^0 = 3.25$ V) permits measurements outside the range of SEI formation reactions, avoiding complications with simultaneous formation of the SEI and intercalation of lithium. In previous work, we developed both rotating disk electrode (RDE) and electrochemical impedance spectroscopy (EIS) techniques to characterize the SEI using ferrocene as an electrochemical probe of the SEI.[1,2] These two approaches have their advantages and disadvantages. The SEI creates both transport and kinetic resistances to reaction, and the RDE method can separate these, unlike impedance. Cyclic voltammetry (CV) has similar limitations, in which the effects of transport and kinetic resistances may be experimentally indistinguishable.[3,4] However, both EIS and CV are much less experimentally demanding and are more suitable for studying different surfaces.

Applying the methods developed in Refs. 1 and 2 to study different surfaces is highly desirable because previous work has found that graphite orientation strongly affects SEI formation reactions. Both Hirasawa et al. and Chu et al. used AFM images of highly oriented pyrolytic graphite (HOPG) to find that film formation began preferentially along cleavage steps of the HOPG surface and crystal boundaries of a composite graphite electrode between 1.5 and 2.0 V. Reduction occurred on the basal plane of HOPG and the surface of the composite electrode at 0.8 to 0.9 V.[5,6] In these studies, the HOPG orientation was controlled by imaging either a cleavage step on the electrode or an area of the electrode that contained no defects; thus, separately attributing macroscopic electrochemical properties to the different SEIs formed on the edge and basal plane of graphite was not possible. Yamada et al. took a different approach by measuring the fraction of edge planes on the HOPG surface using the kinetics of $Ru(NH_3)Cl_6$ and showing that it was inversely proportional to the macroscopic charge-transfer resistance for lithium-ion intercalation.[7] A similar result was found in a series of papers from Novak's group. Using temperature desorption experiments, they measured the active surface area, which is correlated to defects in the graphite structure. Cycling experiments then showed that, for a higher concentration of defects, electrolyte decomposed faster, permitting reversible intercalation instead of cointercalation and graphite exfoliation.[8,9]

In this work, both CV and EIS of ferrocene are used to monitor the electronic passivity of HOPG as the SEI is formed. We combine the techniques of Refs. 1, 2, 7 and 10 to relate the fraction of exposed edge planes on graphite, f_e, to macroscopic passivation properties. We also study the effects of SEI formation voltage and compare behavior in $LiPF_6$-based and $LiClO_4$-based electrolytes.

Experimental

Grade ZYH HOPG (mosaic spread 3.5 ± 1.5) was obtained from Momentive Performance Materials Quartz, Inc. and Structure Probe, Inc. and cleaved with adhesive tape before use. Cleavage exposed primarily the basal plane, with a fraction of edge planes, f_e along grain boundaries and defects. f_e is here defined as the fraction of total electrode area that exposes the edge plane to the electrolyte. f_b, the fraction of total electrode area that exposes the basal plane to the electrolyte, is equal to $1 - f_e$. Isolating the edge plane by embedding HOPG in resin is difficult because cutting and polishing the graphite introduces many irregularities into the system. The pressure of polishing may also cause graphite lamellae to fold and bend, exposing basal planes instead of edges. To avoid this time- and material-intensive method, samples with high values of f_e were prepared by finely scratching the freshly-cleaved HOPG surface with a sharp tweezer tip to create many surface defects. A commercially available glassy carbon electrode (BASi, Inc) was prepared using the procedure developed in Ref. 1.

The fraction of edge plane, f_e, was determined from the double-layer capacitance C_{dl}, which has been shown to increase with an increasing ratio of edge to basal planes.[11] Because C_{dl} in HOPG is

* Electrochemical Society Student Member.
** Electrochemical Society Active Member.
*** Electrochemical Society Fellow.
z E-mail: mtang@berkeley.edu.

Downloaded on 2014-08-27 to IP 130.54.130.242 address. Redistribution subject to ECS terms of use (see ecsdl.org/site/terms_use) unless CC License in place (see abstract).

京都大学 KYOTO UNIVERSITY
A Self-archived copy in
Kyoto University Research Information Repository
https://repository.kulib.kyoto-u.ac.jp
京都大学学術情報リポジトリ KURENAI 紅 Kyoto University Research Information Repository

the capacitance of the space charge layer within the graphite instead of the diffuse part of the electrolyte double layer, values of C_{dl} can be distinguished into $C_{dl,e}$ and $C_{dl,b}$, based on the different electronic structures of the edge and basal planes, respectively.[12] Cyclic voltammagrams were measured in neat 1.0 M KCl with a Ag/AgCl reference and platinum counter electrode, and C_{dl} was calculated from the variation of average current with scan rate. The potential limits were ±50 mV from the open-circuit potential, and the scan rate ranged from 100 to 5000 mV/s. For HOPG, the electrode area was fixed at either 0.2893 or 0.5024 cm^2 with an O-ring. Cells were made of Teflon or polypropylene. For glassy carbon, a commercially available glass cell was used. f_e was also measured using the method of Nicholson to extract a rate constant for the reaction of 1.0 mM $Ru(NH_3)_6Cl_3$ in 1.0 M KCl. Although this method has been used by several other groups,[10,13] the scratched HOPG samples exhibited reversible kinetics, so that accurate extraction of a rate constant was not possible.

After measuring the fraction of edge planes, the cell was dried in a 60°C oven without removing the HOPG electrode and introduced to an argon atmosphere for SEI formation experiments. Care was taken to ensure that the cell temperature equilibrated to the glovebox temperature of 22–25°C. Lithium foil was used for the counter and reference electrodes. Electrolytes tested were 1.0 M $LiClO_4$ in ethylene carbonate (EC): dimethyl carbonate (DMC) (1:1 volume, Kishida Chemical), 1.0 M $LiClO_4$ in ethylene carbonate (EC): diethyl carbonate (DEC) (1:1 weight, Kishida Chemical), or 1.0 M $LiPF_6$ in EC:DEC (1:1 weight, Novolyte). Approximately 2.0 mM ferrocene (Sigma) was added to the electrolyte for some experiments. Instrumentation was a either a 1480 Multistat with Corrware software (Solartron) or a VMP potentiostat with EC-Lab software (BioLogic).

Results and Discussion

Determination of f_e.— Double-layer capacitance was measured by cycling the electrode about the open-circuit potential at 100 to 5000 mV/s. The slope of the steady-state current versus scan rate gives the double layer capacitance, which is related to f_e by

$$C_{dl} = C_{dl,e} f_e + C_{dl,b}(1 - f_e) \quad [1]$$

The values for $C_{dl,e}$ and $C_{dl,b}$ used were 60 and 2 μF/cm^2.[11] A plot of f_e as calculated from Eq. 1 is shown in Fig. 1. Circles represent samples that were merely cleaved, while stars mark the samples that were scratched to increase the percentage of edge sites. The calculated values of f_e generally range between zero and unity, although several data points are outside this range. Values greater than unity or less than zero are not physically meaningful. However, any uncertainty in the values of $C_{dl,e}$ or $C_{dl,b}$ will affect the calculated values of f_e. Rice, et al. reported that $C_{dl,e}$ could range up to 150 μF/cm^2, depending on the electrode surface treatment. Using a reference value of $C_{dl,e}$ = 150 μF/cm^2 brings the calculated values of f_e in Fig. 1 within the range of 0 to 1. The emphasis in this work is not the quantitative relationship between C_{dl} and f_e, but the qualitative effect of f_e on the formation and passivation properties of the SEI. Thus, because of the uncertainty in $C_{dl,e}$, measuring C_{dl} serves the present purpose of providing a qualitative, but not a quantitative, indicator of f_e.

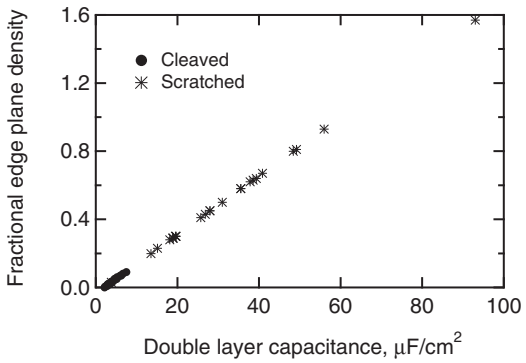

Figure 1. Calculation of f_e from double-layer capacitance. Dots are samples that are cleaved, stars are samples that were deliberately scratched to increase the number of defects and grain boundaries.

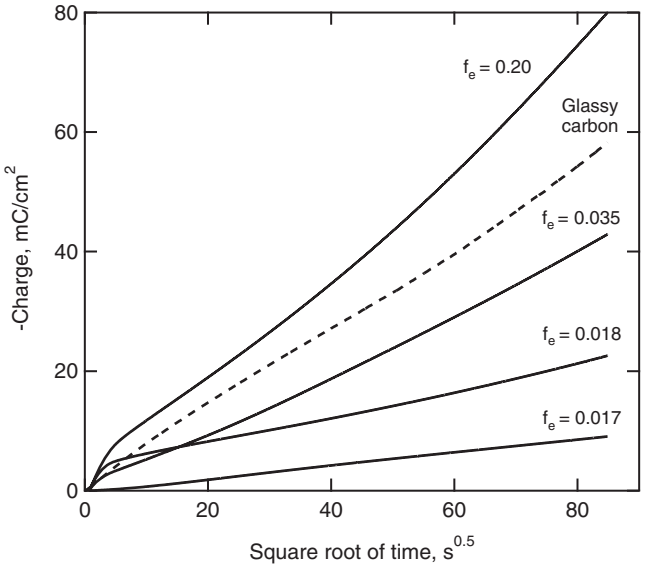

Figure 2. Potentiostatic SEI formation on HOPG at 0.6 V vs. lithium. As f_e increases, the rate of growth increases although the shape of the curve does not change. The dotted line shows SEI formation on glassy carbon under the same conditions. Charge is negative because SEI formation is a reduction process.

Potentiostatic SEI growth.— An SEI was formed by holding the HOPG electrodes at 0.6 V vs. Li/Li^+ in $LiClO_4$ EC:DEC for 120 minutes. Total charge passed as a function of time is plotted for selected trials in Figure 2. Plotting charge versus the square root of time gives a straight line, suggesting transport-limited growth. There are two distinct regions to each curve, with a transition time at approximately 20 seconds. The slope of the short-time growth region is greater than the slope at long times for all curves. Plotting the best-fit slope of each region versus f_e shows that, at long times, the SEI growth rate increases with fraction of edge planes (Fig. 3). At short times, measurements are more sensitive to instrument error, and the trend with f_e is less clear. The definition of t = 0 is also uncertain.

A higher reaction rate with increased f_e suggests that SEI-formation reactions are surface-specific and require edge sites to intercalate partially before electrochemical decomposition;[14] however, cointercalation is not required to explain the trend. If SEI formation reactions begin at higher potentials along the edge than the basal plane, formation at the same voltage of 0.6 V will result in a higher driving force, and thus higher reaction rate, on the edge plane. Furthermore, for the experiment described in Fig. 2, lithium intercalation should be occurring simultaneously. Because lithium ions intercalate only at the edge sites of graphite, the trend of the slope of Q vs. $\sqrt{t}$ with f_e may also be explained independently of any SEI formation.

In order to compare SEI formation on different types of carbon, the same potentiostatic SEI formation experiment was repeated on a glassy carbon electrode; this curve is shown by the dashed line in Fig. 2. The straight line shows that SEI formation on glassy carbon also exhibits parabolic growth. The magnitude of current is also similar between the two materials. These two observations suggest that glassy carbon may be used as a model surface for SEI formation, as previous studies have done.[1,2] However, the dependence of formation rate on f_e in Fig. 3 points to the importance of knowing the fractional edge-plane density. Measuring the capacitance on glassy carbon in aqueous KCl shows that f_e is much lower than the value of f_e predicted by the relationship in Fig. 2 and the measured rate of SEI formation (triangles,

Downloaded on 2014-08-27 to IP 130.54.130.242 address. Redistribution subject to ECS terms of use (see ecsdl.org/site/terms_use) unless CC License in place (see abstract).

京都大学 KYOTO UNIVERSITY
A Self-archived copy in
Kyoto University Research Information Repository
https://repository.kulib.kyoto-u.ac.jp
京都大学学術情報リポジトリ KURENAI 紅 Kyoto University Research Information Repository

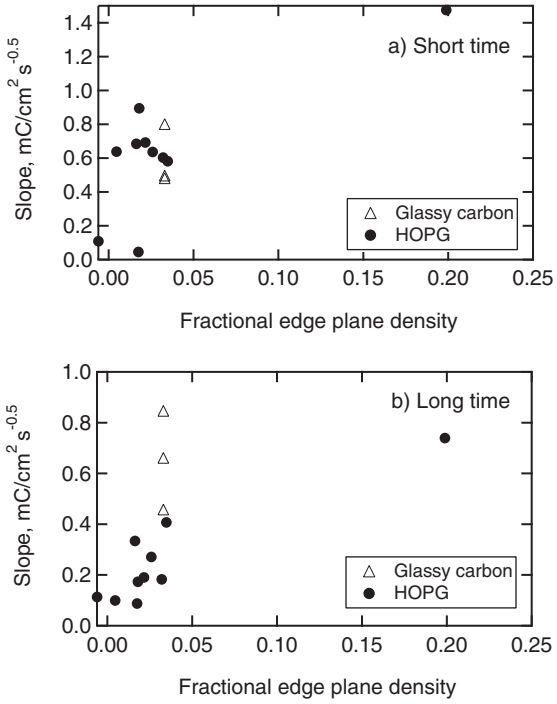

Figure 3. SEI formation slope vs. f_e. The dependence of long-time data on f_e is stronger than that at short time. Formation on glassy carbon (triangles) seems anomalously high, considering the f_e measured. For visual clarity, the y-axes of a) and b) have different scales.

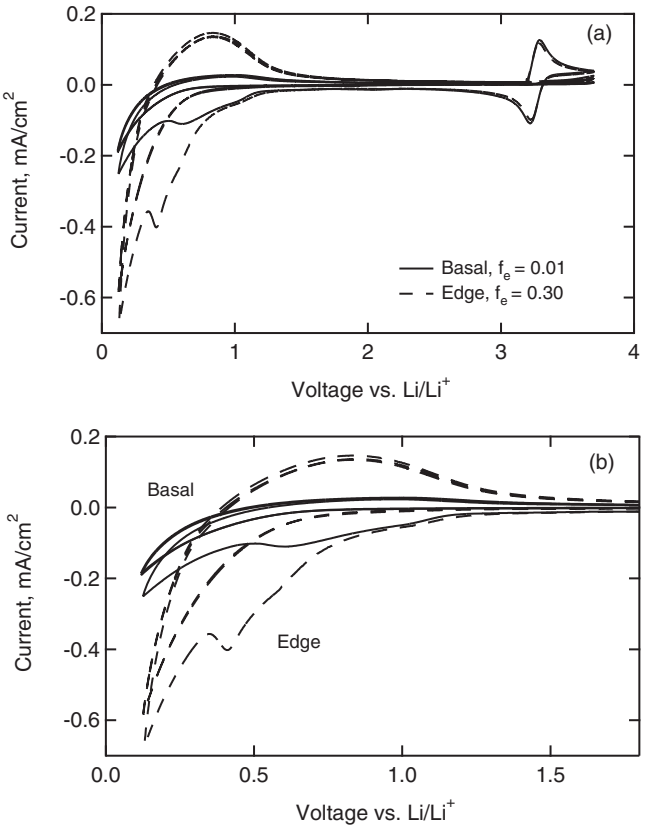

Figure 4. SEI formation in 1:1 EC:DMC 1.0 M $LiClO_4$ on edge and basal planes. Activity is higher on the edge than the basal plane. (a) shows the entire range of data, while (b) zooms in on the SEI-formation-potential region. Scan rate is 20 mV/s.

Fig. 3). The different structure of HOPG means that the reference values of $C_{dl,e}$ and $C_{dl,b}$ used for HOPG may not apply to glassy carbon. Furthermore, the electrochemical behavior of glassy carbon is known to be affected by physi- and chemisorbed impurites.[3,15,16] The cycling procedure used to clean the glassy carbon electrode should remove such impurities, but contact with air or aqueous solution may reintroduce them to the surface. Thus, measuring C_{dl} is probably not an appropriate method of estimating f_e on glassy carbon.

The trend in Fig. 3b agrees with the literature in suggesting that f_e critically affects SEI formation reactions.[5,6] However, the scatter and the difficulty of accurately measuring f_e shows that quantitative analysis of the potentiostatic data in Fig. 2 is extremely difficult without a separate, nonelectrochemical measurement of f_e.

Potentiodynamic SEI formation and ferrocene characterization.— To address the problem of simultaneous intercalation and film formation reactions, and to gain more information about the separate reactions occurring on different orientations of graphite, a potentiodynamic method of SEI formation was implemented. Because lithium intercalation and electrolyte reduction occur at different peak potentials, and because intercalation appears on every cycle while electrolyte reduction decreases with cycling, potentiodynamic methods permit qualitative separation of the different reactions at the HOPG surface. Cells were cycled from open circuit to 3.7 V, then to 0.1 V vs. Li/Li^+ at 20 mV/s. Approximately 2 mM ferrocene was also added to the electrolyte in order to monitor the degree of electronic passivation at the surface. Replicates were performed for each experiment, and while the exact peak voltages and currents varied, the general location and relative magnitudes of the peaks were consistent among samples. The comparison between samples of high fractional basal plane (cleaved samples) and high fractional edge plane (scratched samples) was also generally consistent. Control cyclic voltammagrams in neat electrolyte without ferrocene were consistent, indicating the cathodic stability of ferrocene at low potentials.

Fig. 4 shows a representative experiment in $LiClO_4$-based electrolyte. Three cyclic voltammagram cycles are shown on HOPG with a high fractional basal plane ($f_e = 0.01$, cleaved) and a high fractional edge plane ($f_e = 0.30$, scratched). (a) shows the entire range of data, while (b) expands the potential region in which SEI-formation reactions occur. The voltage is corrected for ohmic drop by

$$E_{cor} = E_{meas} - i R_b \quad [2]$$

where the bulk electrolyte resistance, R_b, is measured before SEI formation using AC impedance. Although R_b may change as the SEI evolves, the voltage correction should be the most accurate on the first cycle of formation, when most of the SEI formation occurs.

On both samples, the reduction peak at 0.1 V and oxidation peak at approximately 0.9 V occur on all cycles and thus correspond to lithium intercalation and deintercalation. Additional reduction peaks at 1.0 V and 0.45 V (on the edge plane) or 0.6 V (on the basal plane) are visible only on the first cycle and thus correspond to SEI formation. All three peak currents are higher on the edge than the basal plane. After the SEI is formed, the steady-state intercalation and deintercalation currents should increase linearly with f_e because lithium intercalates preferentially or even exclusively at edge sites. Because SEI formation takes place on both orientations, it is not expected to scale so directly. Fig. 4 shows that, although f_e increases by a factor of 30 between the two samples, the peak intercalation and deintercalation currents increase by factors of approximately three and seven, respectively. The SEI formation peak at 0.45 or 0.6 V increases by a factor of approximately four. The discrepancy between the expected ratio of 30 and the measured ratio of seven may reflect inaccuracy in the absolute measurement of f_e, or simply that, for complicated reactions such as intercalation and electrolyte decomposition, simple linear relationships do not apply. The experiment in Fig. 4 was repeated over multiple trials. Although all three peak currents generally increased with f_e, the scatter in the data was too great to determine a definite

Downloaded on 2014-08-27 to IP 130.54.130.242 address. Redistribution subject to ECS terms of use (see ecsdl.org/site/terms_use) unless CC License in place (see abstract).

京都大学 KYOTO UNIVERSITY
A Self-archived copy in
Kyoto University Research Information Repository
https://repository.kulib.kyoto-u.ac.jp
京都大学学術情報リポジトリ KURENAI 紅 Kyoto University Research Information Repository

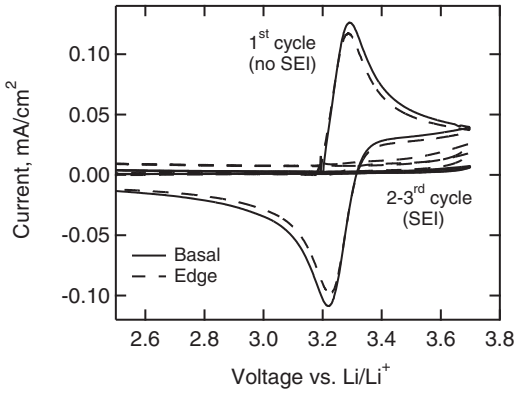

Figure 5. Effect of SEI formation on ferrocene CV in 1.0 M $LiClO_4$ in EC:DMC. Before formation, the ferrocene reaction is fast. After one formation cycle to 0.1 V, electron transfer is almost entirely prevented. Despite higher SEI-formation currents on the edge plane, more ferrocene reaction occurs through the SEI on the edge plane.

shape of the relationship between peak current and f_e in any of the cases.

The effect of the SEI on ferrocene oxidation and reduction is also shown in Fig. 5, which is an expanded view of the high-voltage behavior in Fig. 4a. Before SEI formation and after correcting for ohmic drop, the peak potential separation is 73 mV on the basal plane and 66 mV on the edge plane, close to the reversible limit of 59 mV. The peak currents differ on the electrodes by approximately 8%, suggesting that scratching the electrode to expose more edge sites does not increase the microscopic electrode area because of surface roughening. After only one cycle of formation, the CV shows almost no ferrocene oxidation and reduction on the basal plane, and a very small current on the edge plane. Thus, the SEI formed on both orientations is almost completely electronically passivating after the first cycle, but the edge plane shows slightly higher activity, despite larger SEI formation currents and thus, presumably, a more completely passivated electrode. The slightly higher current in Fig. 5 may indicate that the edge-plane SEI is less electronically insulating than the basal-plane SEI, or simply that higher electronic activity on the edge plane permits greater activity, despite a thicker SEI. In Fig. 6, impedance spectra on the edge plane before and after the cycling experiment in Fig. 4 also show the complete electronic passivation of the SEI after formation cycles. Before cycling (dashed line), the lack of a high-frequency semicircle also shows that the reaction is fast. After formation, the impedance is extremely large. While the spectrum may

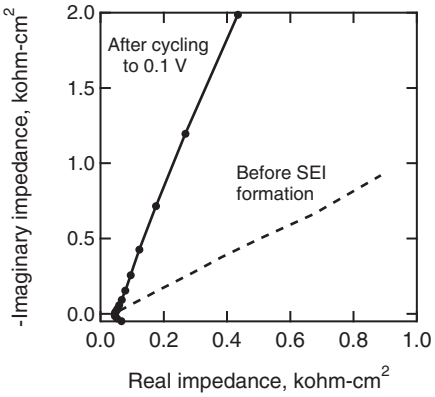

Figure 6. Effect of SEI formation on ferrocene CV in 1.0 M $LiClO_4$ in EC:DMC. After three formation cycles to 0.1 V, the width of the high-frequency arc increases from a negligible amount to a number outside the range of measurement. Data shown is from the edge-plane sample in Fig. 4.

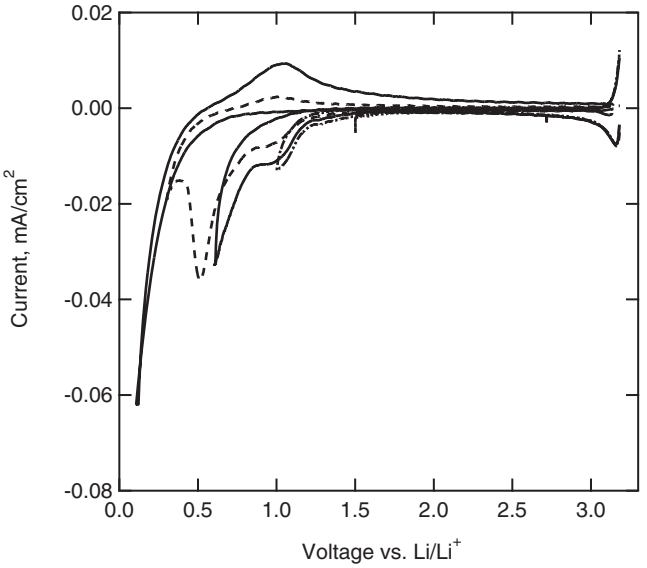

Figure 7. SEI formation CV in 1.0 M $LiClO_4$ in EC:DMC, cycling to variable voltage limits at 10 mV/s. Location of peaks is the same as in Fig. 4. For visual clarity, the y-axes have different limits. $f_e = 0.02$.

exhibit a high-frequency semicircle, the diameter of the semicircle is too large to be captured in the accessible frequencies.

Effect of formation voltage.— Figs. 4 and 5 show that passivation in $LiClO_4$-based electrolyte is almost entirely complete after one formation scan to 0.1 V. In order to form the SEI at a slower rate and monitor its development by ferrocene kinetics, the electrode was cycled to progressively lower voltages. In between formation scans at 10 mV/s, EIS was measured at open circuit (E^0 = 3.2 V), and a ferrocene CV taken between 2.5 and 3.7 V at a scan rate of 100 mV/s.

This experiment is shown in Fig. 7 on a sample of primarily basal plane (f_e = 0.02). The electrode was cycled from open circuit at 3.2 V to 2.1, 1.5, 1.0, 0.6, 0.3, and 0.1 V, in that order, at 10 mV/s. SEI formation peaks occur at approximately 1.0 and 0.5 V, in agreement with Fig. 4. Residual oxidation and reduction of the ferrocene couple is seen at 3.2 V. Because the scan rate is slower, the magnitude of current is much smaller. Although SEI formation peaks begin to occur at 1.0 V, ferrocene kinetic measurements as shown in Fig. 8 show that the SEI does not provide electronic passivation until the formation voltage decreases below 0.6 V. Until the formation voltage decreases below 0.6 V, the ferrocene cyclic voltammagram does not deviate from that measured before the SEI formation cycles. The dashed line showing the ferrocene current before SEI formation is hidden underneath curves measured after formation, showing the complete lack of electronic passivation above 0.6 V. After formation to 0.3 V, the ferrocene reaction is almost completely suppressed. The CV after formation to 0.3 V shows a small oxidation current as potential reaches 3.7 V. Although this current could be ferrocene oxidation, it could also be oxidative stripping of the SEI, which occurs above 3.5 V on glassy carbon.[1,17] The large oxidation peaks in Fig. 8 at 3.2 V are artifacts of the cycling protocol, which was defined in terms of the open-circuit potential. Because the relative concentrations of ferrocene and ferrocenium at the surface varied with time and potential, E^0 drifted during experiments. Although the drift was typically less than 20 mV, it caused the potentiostat to apply an abrupt step change in the potential at the start of the diagnostic CV and, thus, to measure a large and rapidly decaying current due to double-layer charging. Although the magnitude of the current at 3.2 V in Fig. 8 is high, it decays rapidly, in a manner consistent with double-layer charging. Furthermore, the curves measured after formation above 0.6 V show no changes to either the potential or magnitude of the peak ferrocene

Downloaded on 2014-08-27 to IP 130.54.130.242 address. Redistribution subject to ECS terms of use (see ecsdl.org/site/terms_use) unless CC License in place (see abstract).

京都大学 KYOTO UNIVERSITY
A Self-archived copy in
Kyoto University Research Information Repository
https://repository.kulib.kyoto-u.ac.jp
京都大学学術情報リポジトリ KURENAI 紅 Kyoto University Research Information Repository

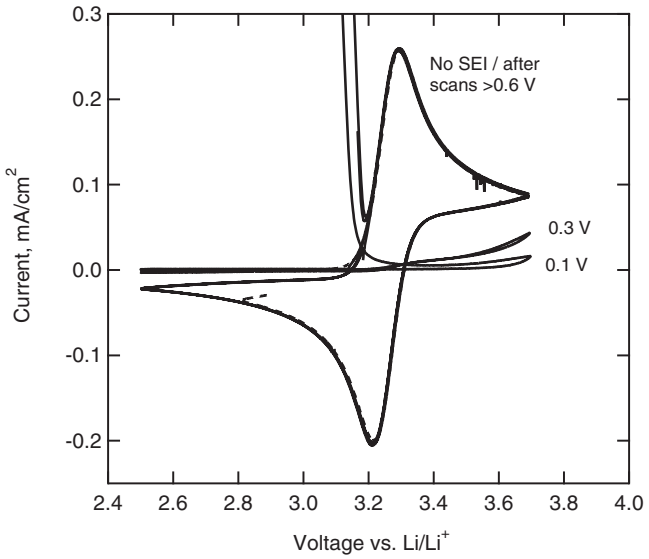

Figure 8. Effect of SEI formation on ferrocene CV in 1.0 M $LiClO_4$ in EC:DMC, variable formation voltage. No change in through-film ferrocene reaction is seen until the formation voltage decreases below 0.6 V, after which the ferrocene reaction is almost entirely suppressed. The dashed line showing the ferrocene current before SEI formation is hidden underneath curves measured after formation, showing the complete lack of electronic passivation above 0.6 V.

current, indicating that the current is non-faradaic and does not affect the ferrocene measurement.

The Nyquist plot in Fig. 9 corroborates the difference between SEI formation above and below 0.6 V. The impedance before SEI formation is shown by the dashed line in (a). The 45° slope and lack of high-frequency semicircle show a fast reaction. After SEI formation, EIS spectra show a similarly fast reaction until after the formation cycles to 0.3 V and 0.1 V, when the charge-transfer resistance rapidly increases (Fig. 9b). Although the charge-transfer resistance increases greatly after SEI formation, the real intercept at high frequency does not increase with cycling. The rapid changes in the ferrocene CV and EIS measurements between formation to 0.6 and 0.3 V show that, even though the SEI begins to form at 1.0 V in $LiClO_4$-electrolyte (Fig. 7), it does not provide electronic passivation until the formation voltage decreases below 0.6 V, upon which it blocks electron transfer very rapidly. It is unclear from the experiments whether the difference above and below 0.6 V is caused by a difference in reaction products or simply because the formation reactions have not occurred enough to cover the electrode.

Effect of solution contamination.— In this study, water contamination was a major concern because f_e was measured using aqueous KCl. In order to keep a constant electrode area, the cell was not disassembled while drying. Thus, although the electrolytes used were battery-grade chemicals with extremely low water content, trapping water in the O-ring during cell drying remained a possibility. Aurbach, et al. found that water reduction occurs in nonaqueous electrolytes at approximately 1.5 V vs. lithium.[18] Although the SEI formation spectra in Figs. 4 and 7 do not show any clear peaks at this potential, the high scan rate employed (20 mV/s) may cause irreversible reactions such as water reduction to begin at lower potentials. Thus, the reduction processes in Figs. 4 and 7 beginning at approximately 1.0 V may involve the reduction of trace water as well as electrolyte.

While the use of aqueous solutions in this work suggests that water is a possible contaminant, reduction of oxygen to is also known to occur between 2.1 and 1.6 V vs. lithium.[18] Fig. 10 shows an experiment in which a 1.9 V reduction peak is observed. This peak occurred unpredictably and was not correlated to C_{dl} or f_e, suggesting a contaminant, and the location of the peak at 1.9 V suggests oxygen. The

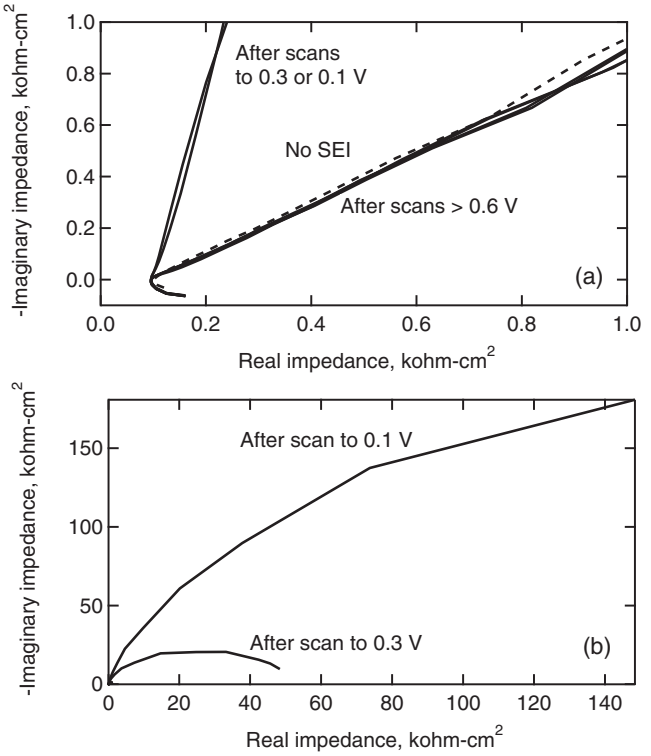

Figure 9. Effect of SEI formation on ferrocene CV in 1.0 M $LiClO_4$ in EC:DMC, variable formation voltage. EIS shows an extremely fast reaction on the clean HOPG electrode and until the formation voltage decreases below 0.6 V. The real intercept does not increase with SEI formation.

electrode in Fig. 10 was cycled to 1.2, 0.9, 0.6, 0.45, 0.3, and 0.1 V vs. Li/Li^+. Comparing Figs. 8 and 9 with Figs. 11 and 12 shows how oxygen causes HOPG to become passivated more quickly. When the 1.9 V peak is present, SEI formation current is generally larger at all voltages. Ferrocene current begins to decrease immediately after SEI formation cycling to 1.2 V, whereas the ferrocene CV in Fig. 8

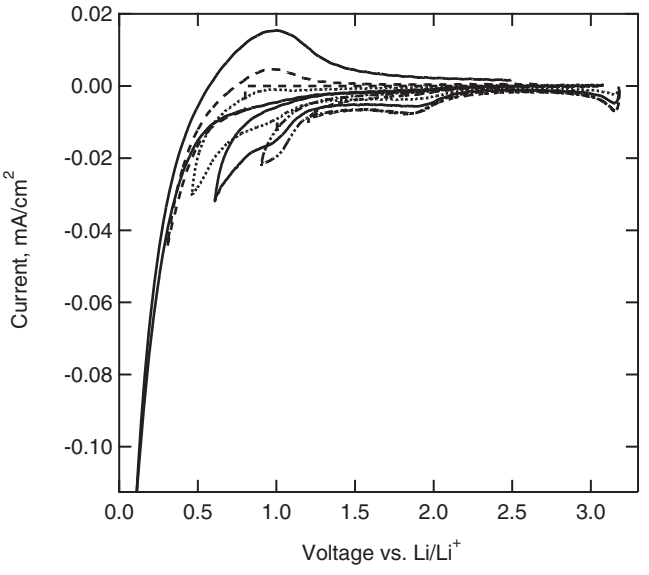

Figure 10. SEI formation CV in 1.0 M $LiClO_4$ in EC:DMC, 10 mV/s. The 1.9 V reduction peak indicates oxygen contamination. Formation currents are higher at all currents than they are in the absence of the 1.9 V peak as in Fig. 7. $f_e = 0.002$.

Downloaded on 2014-08-27 to IP 130.54.130.242 address. Redistribution subject to ECS terms of use (see ecsdl.org/site/terms_use) unless CC License in place (see abstract).

京都大学 KYOTO UNIVERSITY
A Self-archived copy in
Kyoto University Research Information Repository
https://repository.kulib.kyoto-u.ac.jp
京都大学学術情報リポジトリ KURENAI 紅 Kyoto University Research Information Repository

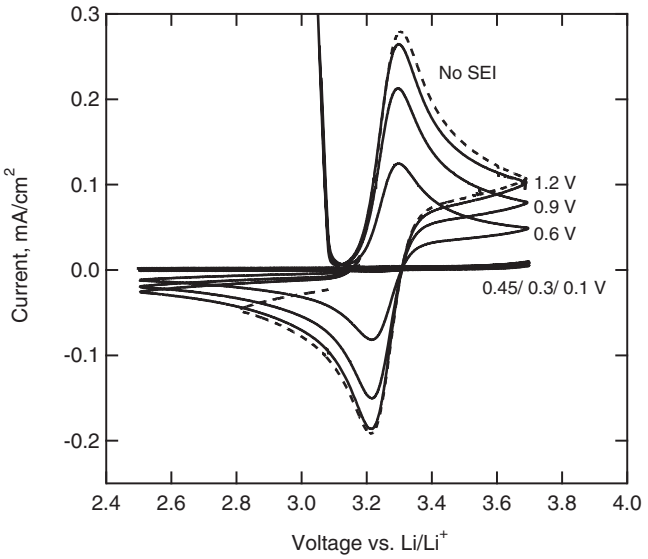

Figure 11. Effect of SEI formation on ferrocene CV in 1.0 M $LiClO_4$ in EC:DMC, oxygen contamination. In comparison to Fig. 8, the through-film ferrocene current decreases at all formation voltages, showing that HOPG is passivated more rapidly when the contaminant is present.

shows no effects until 0.6 V. EIS data show a similar effect; the rise in charge-transfer resistance occurs earlier and more rapidly in contaminated electrolytes. EIS also shows that, as more SEI is formed, the real intercept increases from 0.0995 to 0.1052 kohm-cm^2. Thus, the reaction products formed in the presence of the contaminant are more ionically, as well as electronically, resistive. These observations are consistent with the predicted products of either oxygen or water reduction. In carbonate solvents, McCloskey, et al. found that the primary product of oxygen reduction was Li_2CO_3, while Aurbach found that water was reduced to LiOH.[18,19] Both compounds should be both less soluble (and thus more passivating) and less ionically conductive than polymer-like reduction products of the carbonate solvent.[18,20] Thus, the effects of the contaminant on the ferrocene CV and impedance do not by themselves specify the electrochemical reactions. To accurately identify the reaction products, spectroscopic or other non-electrochemical methods are necessary. Although f_e in Fig. 7 was measured as 0.002, the deintercalation peak at 1.0 V is larger than the basal plane sample in Fig. 4, which has a calculated value of $f_e = 0.02$. However, the measured values of C_{dl} for the two samples differ by less than 1 μF/cm^2, attesting to the difficulty of accurately measuring f_e by this method when f_e is low and C_{dl} is small.

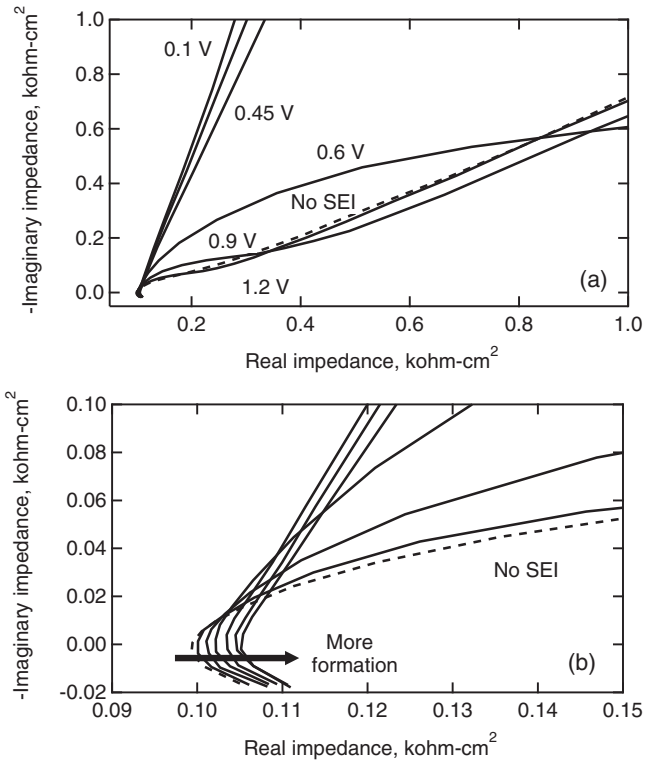

Figure 12. Effect of SEI formation on ferrocene CV in 1.0 M $LiClO_4$ in EC:DMC, oxygen contamination. The rise in charge-transfer resistance occurs earlier and more rapidly than in Fig. 9. Zooming in on the real intercept shows that, reaction products formed in the presence of the contaminant are more ionically, as well as electronically, resistive.

The characteristic parameters of impedance spectra, the high-frequency arcwidth and time constant, provide only a comparative measure of passivation because both kinetic and transport resistances from the SEI affect the parameters in the same way.[2] The characteristic measurements from CV, the peak current height and peak potential separation, can sometimes give mechanistic information about the mechanism of passivation; for example, increased peak splitting is most commonly attributed to a slower rate constant, while a reduced peak current is attributed to a mass-transfer limitation. At formation voltages 0.6 V and higher, the data in Fig. 11 show a decreasing peak ferrocene current, and no change in peak potential splitting. This indicates that the kinetics of the ferrocene reaction do not change, and that the change in current is caused by either a decrease in active area (a partially blocked electrode) or by the formation of a porous layer that slows diffusion. Distinguishing between these two mechanisms from the cyclic voltammagram is difficult, if not impossible. After formation to 0.45 V or lower, charge-transfer in Figs. 8 and 11 is so complete that no peak current or peak potential can be observed. Therefore, the results of Figs. 10 to 12 cannot provide conclusive information about the mechanism of passivation, although they do provide a useful qualitative metric.

Comparison of $LiClO_4$ and $LiPF_6$-based electrolytes.— The potentiodynamic experiment in Fig. 4 was repeated in 1.0 M $LiPF_6$ EC:DEC to compare the effect of fractional edge plane in the presence of a different salt anion. The HOPG electrodes were again cycled from open circuit, to 3.7 V, to 0.1 V vs. lithium three times at 20 mV/s. Fig. 13 shows two representative trials on the basal plane ($f_e = 0.01$) and the edge plane ($f_e = 1.0$). Comparison with Fig. 4 shows that the SEI formation behavior is extremely different between the two electrolytes. On the basal plane, the CV exhibits additional peaks at 0.8 and 0.45 V that are not seen in $LiClO_4$-based electrolyte. Additionally, in $LiClO_4$ solutions, the SEI formation peaks disappear completely after the first cycle, but in Fig. 13 a, the SEI formation peak at 0.45 V is still visible. Further cycling (not shown) was able to suppress the formation peaks and reach a steady-state profile after approximately 8 to 10 cycles. On the edge plane (Fig. 13b), the location of the single peak is similar in the two electrolytes. However, passivation is not completed after a single cycle as it is in Fig. 4, although it appears to be faster on the edge than the basal plane. The slower passivation in $LiPF_6$-based electrolyte may be due to a number of factors. Aurbach, et al. proposed that HF, an unavoidable contaminant in $LiPF_6$-based electrolytes, reacts with and dissolves carbonate reduction products on the electrode surface; such dissolution reactions would slow the rate of SEI formation until more stable products were formed.[21,22] Another possibility is that PF_6^- slows the precipitation kinetics of SEI products, causing slower passivation; the identity of the anion has been shown to affect precipitation kinetics in previous work.[23] The overall magnitude of the SEI formation current on the basal plane is similar in the two electrolytes, consistent with a recent study by Marom, et al., who compared $LiPF_6$ and $LiClO_4$ on platinum electrodes.[22] On the edge plane, the measured SEI formation current is approximately five times higher than that in $LiClO_4$ electrolyte, consistent with the higher value of f_e in Fig. 13b than in Fig. 4b (1.0 vs. 0.30).

Downloaded on 2014-08-27 to IP 130.54.130.242 address. Redistribution subject to ECS terms of use (see ecsdl.org/site/terms_use) unless CC License in place (see abstract).

京都大学 KYOTO UNIVERSITY
A Self-archived copy in
Kyoto University Research Information Repository
https://repository.kulib.kyoto-u.ac.jp
京都大学学術情報リポジトリ KURENAI 紅 Kyoto University Research Information Repository

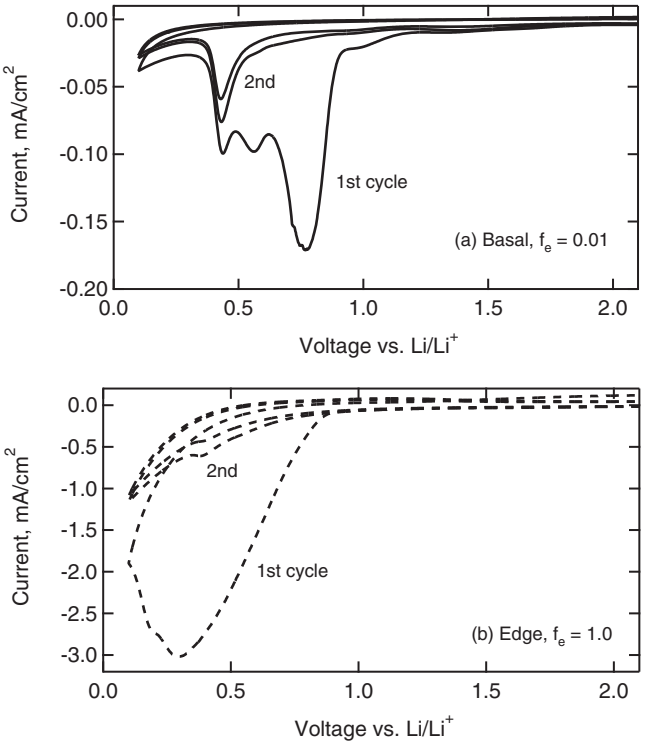

Figure 13. SEI formation in 1:1 EC:DEC 1.0 M $LiPF_6$ on edge and basal planes. (a) shows a sample with $f_e = 0.01$, while (b) shows the edge plane, $f_e = 1.0$. Scan rate is 20 mV/s. The voltammetric response is very different from $LiClO_4$-based electrolyte (Fig. 4), both in the location and magnitude of peaks. Passivation is also much slower.

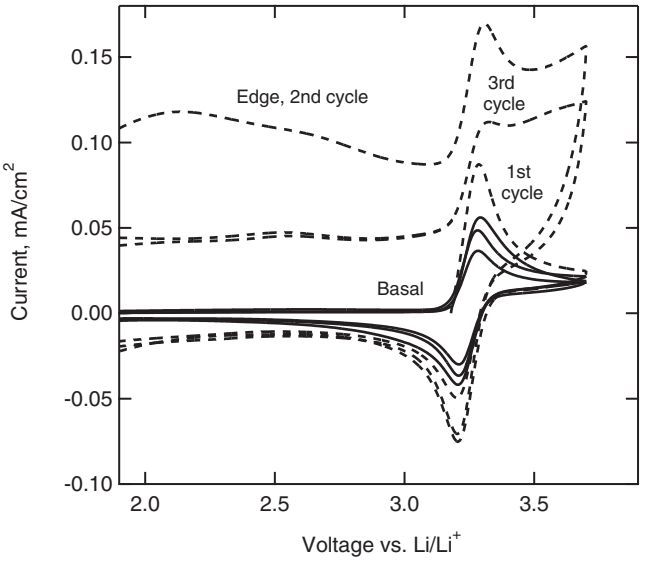

Figure 14. Effect of SEI formation on ferrocene CV in 1.0 M $LiPF_6$ in EC:DEC. On the basal plane, passivation is much slower than in $LiClO_4$-based electrolyte. On the edge plane, the SEI is oxidized at voltages greater than 2.1 V, as shown by currents larger than the reversible ferrocene current. Because the film is removed in the voltage range of the ferrocene reaction, ferrocene CV cannot be used to compare electronic passivation on the edge and basal planes.

The high-voltage behavior of the experiment in Fig. 13 is shown in Fig. 14. Initially, the peak potential separation for the ferrocene reaction is 77 mV on the basal plane and 65 mV on the edge plane. Ferrocene current is substantially higher on the edge plane, suggesting that, for this trial, scratching the electrode may have increased the microscopic surface area by roughening in addition to exposing more edge sites. However, the ferrocene peak current increases by approximately 55%, while the SEI formation and lithium de/intercalation currents increase by factors of 18 to 120, showing that surface roughness cannot be the only factor influencing the measurements. On the basal plane (solid line), the peak ferrocene oxidation and reduction currents decrease slightly with each cycle, and the peak potential separation remains nearly constant. Although the passivation is much slower than in $LiClO_4$-based electrolyte, the overall behavior is consistent with that in Fig. 11, which shows gradual passivation due to formation of a porous layer or partial blocking of the electrode.

The edge plane, in contrast, shows a dramatically different electrochemical response. On the second cycle, a large oxidation current is seen even below 2.0 V. This current shows a maximum at approximately 2.1 V, then peaks again at the location of the ferrocene peak potential and again at the upper scan limit of 3.7 V. Because the peak current is higher than that observed with no SEI, the oxidation current must correspond to oxidative stripping of SEI products from the electrode. Removal of SEI products explains why the reduction peak for ferrocenium on the second cycle is almost unchanged from that on the electrode without an SEI. As the electrode is cycled a third time, the decreased height of the oxidation and reduction peaks show that the ferrocene reaction is suppressed. Although the high current on the second cycle shows the oxidation of SEI products, the formation peak is still suppressed greatly from the first to second cycle in Fig. 13, showing that the oxidation reaction at high voltage does not completely remove SEI products. The partial removal of the film at high voltages complicates any comparisons between electronic passivation on the edge and the basal planes. The oxidative stripping of the edge-plane SEI in Fig. 14 was observed consistently over seven trials of the experiment. Stripping of the basal-plane SEI was minimal, occurring only to an extent consistent with a small but non-zero value of f_e. Bar-Tow et al. found that edge-plane SEI was richer in inorganic compounds while basal-plane SEI was richer in organic compounds.[24] A possible explanation for the behavior in Fig. 14 is that organic SEI products are oxidatively stabler. Previous work found that the SEI in $LiPF_6$-based electrolyte was also oxidized at high voltages;[1] the oxidative removal of SEI products on the edge, but not basal plane, suggests that electrolyte reduction products formed on glassy carbon are more similar to those formed on the edge plane.

In the previous study, SEI products on glassy carbon were not oxidized until above 3.5 V, whereas Fig. 14 shows oxidation occuring at 2.1 V and higher. The difference betwen this and the previous study may be due to the different nature of the surface, or to the fast scan rate employed for these experiments (20 mV/s) in comparison with the 0.6 V potentiostatic formation in the previous work. We hypothesize that, at faster formation rates, intermediate SEI products do not have time to form stabler compounds and are more easily oxidized than they are during potentiostatic formation. Preliminary experiments found that decreasing the scan rate from 20 mV/s to 2 mV/s decreased the magnitude of the oxidative current, but did not eliminate the stripping reactions. Future work will study in more detail the effect of scan rate on SEI formation and behavior in $LiPF_6$-based electrolyte.

Conclusions

Potentiostatic experiments show that electrochemical activity is higher on the edge than the basal plane of graphite, in agreement with literature results. At a constant potential of 0.6 V vs. lithium, current increases with increasing fractional edge plane density. Plotting formation charge vs. square root of time suggests transport-limited growth, regardless of the value of f_e. Glassy carbon exhibits similar behavior under the same conditions, although the measured value of

Downloaded on 2014-08-27 to IP 130.54.130.242 address. Redistribution subject to ECS terms of use (see ecsdl.org/site/terms_use) unless CC License in place (see abstract).

京都大学 KYOTO UNIVERSITY
A Self-archived copy in
Kyoto University Research Information Repository
https://repository.kulib.kyoto-u.ac.jp
京都大学学術情報リポジトリ KURENAI 紅 Kyoto University Research Information Repository

f_e and the measured rate of film growth are not consistent with the correlation for that on HOPG. During potentiodynamic SEI formation experiments, the edge plane exhibits higher currents for both SEI formation reactions, which appear only on the first cycle, and for lithium de/intercalation currents, which reach a steady-state profile for oxidation and reduction.

Including ferrocene in the electrolyte permits in-situ monitoring of the degree to which an electrode is electronically passivated. In $LiClO_4$-based electrolyte, higher through-film ferrocene currents on the edge plane show that, despite greater SEI formation currents, the film formed on the edge plane is less passivating than that formed on the basal plane. The presence of oxygen contamination leads to an SEI that forms and passivates faster. The SEI forms more slowly in $LiPF_6$ than in $LiClO_4$-based electrolyte. On the edge plane, SEI products of $LiPF_6$ reduction are oxidized at voltages greater than 2.1 V. The difference between $LiPF_6$-based and $LiClO_4$-based electrolytes points to the importance of the anion in passivation behavior.

The CV of ferrocene as the SEI is formed at different voltages shows a decrease in peak current, but no change in peak-potential splitting, indicating either a partially blocked electrode or a transport limit caused by a porous film. Considering the sensitivity of the measurements, conclusive mechanistic analysis to distinguish between a porous-layer model and an active-site model is not possible. Furthermore, the results presented here on SEI formation, which occurs over minutes and hours, may not be directly applicable to SEI growth, which occurs over months and years and is responsible for capacity fade. The possibility that slow passivation in $LiPF_6$-based electrolyte is due to slow precipitation kinetics may also preclude the use of any planar electrode, such as HOPG, for SEI studies. The surface area : electrolyte volume is much higher when using porous electrodes of composite graphite, meaning that reactive intermediates cannot diffuse into a reservoir and will thus reach saturation concentrations and precipitate faster. However, the relative ease of the method and the observations in this work suggest that ferrocene has great utility as a qualitative indicator of electrode passivation in realistic battery systems. Future work will continue to use ferrocene to study the effect of different electrolytes on electrode passivation.

Acknowledgments

This work was supported by the Japan Society for the Promotion of Science Summer Program and the National Science Foundation's East Asia Pacific Summer Institute, as well as the Assistant Secretary for Energy Efficiency and Renewable Energy, Office of Vehicle Technologies of the U.S. Department of Energy under Contract no. DE-AC02-05CH11231. Useful feedback and invaluable translation from S. Takeuchi are gratefully acknowledged.

1. M. Tang and J. Newman, *J. Electrochem. Soc.*, **158**(5), A530 (2011).
2. M. Tang and J. Newman, *J. Electrochem. Soc.*, **159**(3), A281 (2012).
3. C. Amatore, J.-M. Savéant, and D. Tessier, *J. Electroanal. Chem.*, **147**(1-2), 39 (1983).
4. J.-m. Savéant, *J. Electroanal. Chem.*, **302**(1-2), 91 (1991).
5. K. Hirasawa, T. Sato, H. Asahina, S. Yamaguchi, and S. Mori, *J. Electrochem. Soc.*, **144**(4), L81 (1997).
6. A. C. Chu, J. Y. Josefowicz, and G. C. Farrington, *J. Electrochem. Soc.*, **144**(12), 4161 (1997).
7. Y. Yamada, K. Miyazaki, and T. Abe, *Langmuir*, **26**(18), 14990 (2010).
8. P. Bernardo, J. Dentzer, R. Gadiou, W. Märkle, D. Goers, P. Novák, M. E. Spahr, and C. Vix-Guterl, *Carbon*, **49**, 4867 (2011).
9. M. E. Spahr, H. Buqa, A. Würsig, D. Goers, L. Hardwick, P. Novák, F. Krumeich, J. Dentzer, and C. Vix-Guterl, *J. Power Sources*, **153**, 300 (2006).
10. Y. Yamada, Y. Iriyama, T. Abe, and Z. Ogumi, *Langmuir*, **25**(21), 12766 (2009).
11. R. J. Rice and R. L. McCreery, *Anal. Chem.*, **61**(15), 1637 (1989).
12. J.-P. Randin and E. Yeager, *J. Electrochem. Soc.*, **118**, 711 (1971).
13. T. J. Davies, R. R. Moore, C. E. Banks, and R. G. Compton, *J. Electroanal. Chem.*, **574**(1), 123 (2004).
14. J. O. Besenhard, *J. Power Sources*, **54**(2), 228 (1995).
15. R. J. Rice, N. Pontikos, and R. L. McCreery, *J. Am. Chem. Soc.*, **112**(12), 4617 (1990).
16. C. Amatore, J.-M. Savéant, and D. Tessier, *J. Electroanal. Chem.*, **146**, 37 (1983).
17. L. Moshurchak, C. Buhrmester, R. L. Wang, and J. Dahn, *Electrochimica Acta*, **52**(11), 3779 (2007).
18. D. Aurbach, M. Daroux, P. Faguy, and E. Yeager, *J. Electroanal. Chem.*, **297**(1), 225 January (1991).
19. B. McCloskey, D. Bethune, R. Shelby, G. Girishkumar, and A. Luntz, *J. Phys. Chem. Letters*, **2**, 1161 (2011).
20. K. Tasaki, A. Goldberg, J.-J. Lian, M. Walker, A. Timmons, and S. J. Harris, *J. Electrochem. Soc.*, **156**(12), A1019 (2009).
21. D. Aurbach and A. Zaban, *J. Electrochem. Soc.*, **141**(7), 1808 (1994).
22. R. Marom, O. Haik, D. Aurbach, and I. C. Halalay, *J. Electrochem. Soc.*, **157**(8), A972 (2010).
23. D. Aurbach, M. Moshkovich, Y. Cohen, and A. Schechter, *Langmuir*, **15**, 2947 (1999).
24. D. Bar-Tow, E. Peled, and L. Burstein, *J. Electrochem. Soc.*, **146**, 824 (1999).

Downloaded on 2014-08-27 to IP 130.54.130.242 address. Redistribution subject to ECS terms of use (see ecsdl.org/site/terms_use) unless CC License in place (see abstract).